Analysis of Connecting Rod to determine Factor of Safety & Critical Buckling Stress by using Finite Element Method

Saurabh Jain[1] Prof.Pradyumna Viswakarma[2]
[1]M.Tech Student [2]Professor
[2]Department of Mechanical Engineering
[1,2]Radharaman Institute of Research & Technology, Bhopal, India

Abstract— The effective uses of a connecting rod are limited at its maximum strengthening limits. The study was conducted by using the Finite element method. The connecting rod is used with flow of with rotation such as internal combustion engines and reciprocating pumps and compressors. The major study was done on connecting rod by using C70S6 material with different middle thickness &side width. A factor of safety was analyzed and static structural & linear buckling is performed for validation. In our analysis, ANSYS was used and the model was developed on UniGraphics. In order to verify the present ANSYS model, the critical buckling with their deformation by using C70S6 material are compared with the available experimental results present in the literature. And the design of connecting rod with different middle thickness (5.5,5.4,5.3,5.2,5.1) & side width (6.0,6.1,6.2,6.3,6.4). In this study, the simulations of different middle thickness &side width, was analyzed for factor of safety and the configurations of connecting rod are proposed. The results show that increasing side width and decreasing middle thickness increases radius of gyration and factor of safety for each location of connecting rod and decreases the slenderness ratio with increase in a side width simultaneously. The factor of safety of the connecting rod is compared by using four types of profiles i.e. middle thickness (5.5,5.4,5.3,5.2,5.1) & side width (6.0,6.1,6.2,6.3,6.4) of optimized connecting rod for various location.

Key words: Connecting Rod, Factor of Safety, Critical Buckling, Allowable Stress, Finite Element Method

I. INTRODUCTION

In a reciprocal piston engine, the rod connects the piston to the crank or rotating shaft. Alongside the crank, they kind a straightforward mechanism that converts reciprocal motion into rotating motion. Connecting rods may convert rotating motion into reciprocal motion. Traditionally, before the event of engines, they were initial employed in this manner. As a rod is rigid, could transmit either a push or a pull so the rod may rotate the crank through each halves of a revolution, i.e. piston pushing and piston propulsion. Earlier mechanisms, like chains, may solely pull. The earliest proof for a rod seems within the late third century AD Roman Hierapolis sawmills. It additionally seems in two sixth century Japanese Roman saw mills excavated at urban center and Gerasa. The crank and rod mechanism of those Roman watermills converted the motion of the waterwheel into the linear movement of the saw blades. [3] Someday between 1174 and 1206, the Arab creator and engineer Al-Jazari delineated a machine that incorporated the rod with a shaft to pump water as a part of a water-raising machine, however the device was unnecessarily complicated indicating that he still didn't totally perceive the construct of power conversion. In Renaissance European country, the earliest proof of a − albeit automatically misunderstood − compound crank and connecting-rod is found within the sketch books of Taccola. A sound understanding of the motion concerned is displayed by the painter Pisanello (d. 1455) United Nations agency showed a piston-pump driven by a water-wheel and operated by two easy cranks and 2 connecting-rods. The primary steam engines, Newcomen's atmospherically engine, were single-acting: its piston solely did add one direction then these used a series instead of a rod. Their output rocked back and forth, instead of rotating endlessly. Steam engines when these are sometimes double-acting: their internal pressure works on both sides of the piston successively. This needs a seal round the connecting rod then the hinge between the piston and rod is placed outside the cylinder, during a massive slippy bearing block known as a crosshead.

II. TYPES OF CONNECTING ROD

A. Aluminum Connecting Rods

These are CNC machined out of their proprietary. Al alloys are cold extruded but a pair of, 1000 a lot of pressure to make sure consistent grain flow and density. Aluminum Connecting Rods are offered for many any import or domestic applications by providing a totally custom rod at very little or no value on top of that of an "off-the-shelf" product. To be use in high H.P. (1,200 max) and high rate (14,000 max) applications. Because of low fatigue life, once used below high stress things drag athletics solely. Are often use safely with daily driving. Al rods are the most effective alternative for DSM's, sturdy and lightweight.

Fig. 1: Connecting rod made of Aluminum [26]

B. Steel Connecting Rods

Still connecting rods to be employed in moderate to high HP (Forged 900 max, Billet 1200 max) and moderate rate (9500-10,000 max). Appropriate for daily driving, endurance athletics, and drag athletics. Manufacturer makes the best quality steel I beam connecting rods for the DSM. They're appropriate for a multiplicity of applications. A

special shot preening method will increase the fabric density on the part surface, leading to wonderful strength and sturdiness of the ultimate product, from OEM product to high-end race engines.

Fig. 2: Connecting rod made of Steel [26]

C. Titanium Connecting Rods

metal connecting rods to be use in high power unit (1,400 max) and high revolutions per minute (14,000) applications. Maybe use in daily driving, endurance athletics, and drag athletics. Set the benchmark on racetracks round the world. Due to their low weight, they're notably appropriate for top speed Motorsports engines

Fig. 3: Connecting rod made of Titanium [26]

III. LITERATURE REVIEW

H. Grass et.al [2006] - during this investigation a piece items from all stages of the method are won't to examine the pure mathematics, microstructure and native mechanical properties. Combining the results of those examinations with data on native method variables like strain and temperature from numerical simulation created it doable to review the influence of the deformation history on the native microstructure and mechanical properties. The simulation of the new forming method shows sensible agreement with experiments concerning to pure mathematics and temperature fields of the piece of work.

S. Griza et.al [2009] - A finite component Analysis was performed in reference to an analytical fracture mechanics approach progressing to assess the relation between alteration force and fissure propagation in rod bolts. The engine collapse occurred owing to forming laps within the grooves of the bolt shank. Finally, some style enhancements were recommended for avoid future failures: a niche within the groove length at the rod cap interface, enough to avoid combination of forming laps and better stress amplitude; increase of the bolt force assembly to cut back stress amplitude.

Moon Kyu Lee et.al [2010] - The buckling stresses from the recommended FEA approach are nearer to those measured in rig experiments than those from classical formula are. The strain sensitivities to reduction of rod shank are then examined in lights of yield, fatigue and buckling. The strain sensitivity in buckling indicates to be comparatively on top of or similar to those of yield and fatigue. Consequently, once weight reduction of affiliation rod shank is tried, buckling ought to be thought of as a necessary issue in conjunction with the opposite criteria like yield and fatigue.

Liming Zheng et.al [2010] - it absolutely was found that the FEM simulations results showed sensible consistency with the experiments, that indicates that the finite component model is possible and reliable. supported the principal findings from the 2 strategies, optimum ranges of method parameters for various fracture cacophonic connecting rods were foretold, that are a flexibly adjusting notch depth, a curvature radius but zero.08mm and a gap angle among the vary 18–261. The results indicate that the predicting ranges are appropriate for creating sensible SNs that has additionally been proved by the fracture cacophonic experiments.

Vanluu Dao et.al [2012] - With the rise of applied squeeze pressure, the scale of a-Al particles decreases whereas the form issue will increase, that increase the mechanical properties of the connecting-rods. Once the running temperature and die temperature increase, the scale and form issue of primary a-Al particles increase .However, if the die temperature is on top of three hundred 1C, the form issue decreases suddenly. The simplest microstructure and mechanical properties of connecting-rods made-up by SSSC were obtained at the running temperature of 575 1C, die temperature of approximately250 1C, and squeeze pressure of 100MPa.

Saharash Khare et.al [2012] - the hundreds and boundary conditions obtained from the experiments were employed in the finite component model of the rod assembly. A result shows high surface pressure and stresses close to the junction of internet and rim of the rod. The changed style of the rod shows important reduction within the extreme pressure in FEM leading to the many improvement of sturdiness life in laboratory check. A discussion of the spalling drawback has been provided resulting in the affiliation of choose pressure and spalling phenomena.

Xianghui Meng et.al [2012] - The piston dynamics, the oil film and therefore the friction loss of the system square measure analyzed and compared with one earlier model that has been adopted wide. The results on a internal-combustion engine show that the rod inertia will have some influence on the system lubrication yet because the piston dynamics, particularly once engine runs at high speeds.

S.B.Chikalthankar et.al[2012]- Numerical tools are extraordinarily used throughout the rod development part, therefore, the entire perceive of the mechanisms concerned yet because the dependableness of the numerical methodology are extraordinarily necessary to require technological benefits, such as, to cut back project time interval and prototypes price reduction. This work shows the entire rod Finite component Analysis (FEA) methodology. It absolutely was additionally performed a fatigue study

supported Stress Life (SxN) theory, considering the changed clarinetist diagram.

Prof. N.P.Doshi et.al [2013] - Ansys bench module had been used for analysis of rod. We have a tendency to recognize the stresses developed in rod below static loading with totally different loading conditions of compression and tension at crank finish and pin finish of rod. We've additionally styled the rod by machine design approach. Style of rod that by machine design approach is compared with actual production drawing of rod. We have a tendency to found that there's risk of more reduction in mass of rod.

Bai-yan He et.al [2013] - Hardness and tensile tests are performed to verify the mechanical properties of the rod. A nonlinear finite component (FE) analysis with the locked assembly is performed to judge the native stress close to the conjugation faces, and therefore the results shows that the crack position is in step with the high stress spots. As a result, lower yield strength of the fabric and high stress level or high stress concentration are terminated because the main reasons of failure of the rod.

G. naga Malleshwara Rao et.al [2013] - This was entailed by activity an in depth load analysis. Therefore, this study has treated two subjects, first, static load and stress analysis of the rod and second, style optimization for appropriate material to attenuate the deflection. Within the initial of the study the hundreds performing on the rod as a perform of your time square measure obtained. The relations for getting the hundreds for the rod at a given constant speed of crank shaft also are determined. It may be over from this study that the rod may be designed and optimized underneath a comprising tensile load such as 360o crank angle at the most engine speed in concert extreme load, and also the crank pressure because the alternative extreme load. What is more, the prevailing rod may be replaced with a replacement rod manufactured from Genetic Steel.

A. Objective of the Work

The main objective of the current work is:

- Validation of the Ansys models by comparing the present simulated results with the Experimental result of Moon Kyu Lee et.al [3]
- To predict critical buckling at various profiles at constant load of 64.7KN for different middle thickness (5.5,5.4,5.3,5.2,5.1) & side width (6.0,6.1,6.2,6.3,6.4) on connecting rod.
- To simulate the connecting rod of the optimized-section profile having different middle thickness and side width for constant load.
- Buckling sensitivity prediction of connecting rod.
- To define average critical buckling stress, slenderness ratio, radius of gyration, factor of safety, allowable stress for the connecting rod of the different optimized-section profile at constant load.
- To predict factor of safety along the connecting rod.

B. Problem Formulation

The study of various literatures we analyzed the slenderness ratio and failure is higher as compared to present study. The purposes of this study reduce the slenderness ratio, failure and to increase the radius of gyration and factor of safety at static load of 64.7 KN. Thus optimized middle thickness (5.5,5.4,5.3,5.2,5.1) & side width (6.0,6.1,6.2,6.3,6.4) of connecting rod in place of I-section connecting rod.

IV. FINITE ELEMENT METHOD

FEA stands for Finite Element Analysis and as the name suggest the methodology involves the analysis of finite elements. The whole model is divided into number of finite elements and then all the forces and boundary conditions are applied on these finite elements, and then the results of all these finite elements are combined together to give the output of whole model. For example if a line is representing a beam and we have to analyze that beam as a cantilever then FEA will divide this line representing a beam into number of small segments known as element. Then the effect of boundary condition and forces is studied on each segment and the resultant output is the summation of each segment. FEA analysis can help engineers to analyze complicated models. With the development of computer systems FEA has increased to gain importance, since it saves time and money both.

A. Basic Steps Involved In FEA

Meshing of structure is done to analyze the model, which involves the division of structure into small finite elements. Simple polynomial shape functions and nodal displacements are used to determine the overall displacement. Unknown nodal displacements are used to determine strains and stresses developed. From this, the equations of equilibrium are assembled in the matrix form which can be easily be programmed and solved through a computer program. After applying the boundary conditions and loads, nodal displacements are found by solving the matrix stiffness equation. After the nodal displacements are known, element stresses and strains can be calculated.

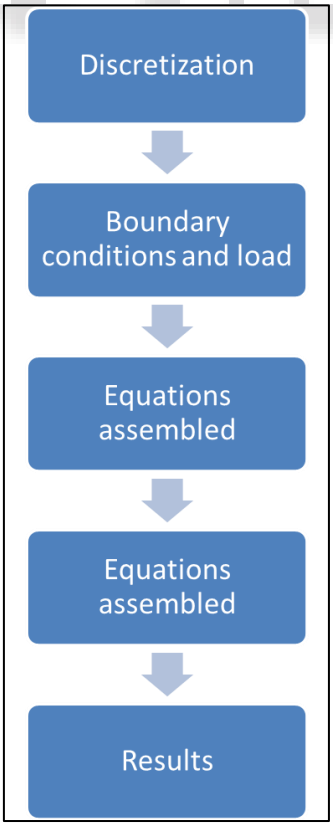

Fig. 4: Block diagram of FEA process

V. MODELING AND ANALYSIS

The procedure for solving the problem is:

- Create the geometry.
- Mesh the domain.
- Set the material properties and boundary conditions.
- Obtaining the solution

Finite Element Analysis of connecting rod :Analysis Type- Static Structural & Linear Buckling Analysis (Coupled field)

Design Parameter	Initial Value(mm)
Frontal profile	
Diameter of small bore (D1)	31
Diameter of big bore (D2)	49
Effective length (L)	140
Shank length (Ls)	57
Shank section	
Fillet radius 1 (R1)	1.0
Fillet radius 2 (R2)	3.5
Total width (L1)	26
Side width (L2)	6.0
Total thickness (T1)	15
Middle thickness (T2)	5.5

Table 1: Dimension of Connecting rod (All Dimensions in mm)

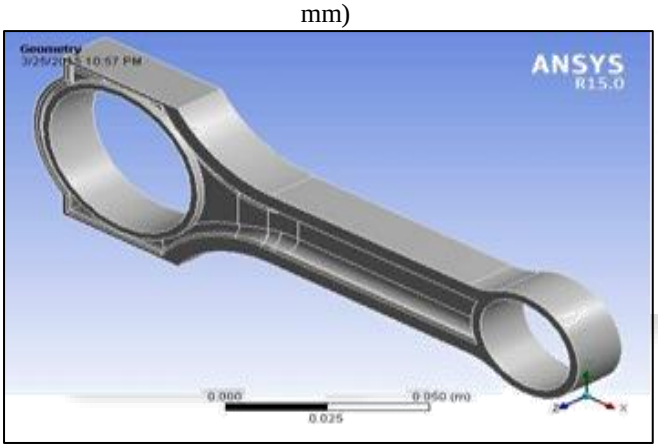

Fig. 5: CAD Model of Connecting Rod width 26mm

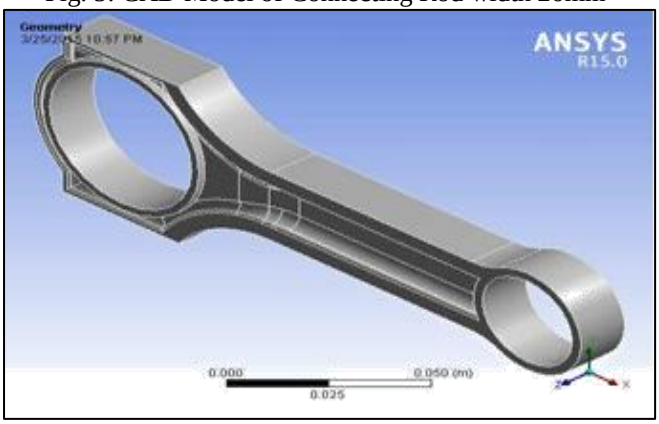

Fig. 6: Model of Connecting Rod width 25mm

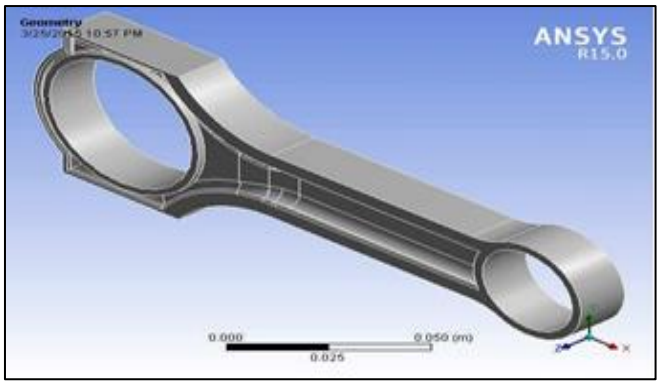

Fig. 7: CAD Model of Connecting Rod width 24mm

A. Design Parameters of Optimized Connecting Rod

Optimized Dimensions	
Middle Thickness	Side Thickness
5.5	6
5.4	6.1
5.3	6.2
5.2	6.3
5.1	6.4

Table 2: Optimized Dimensions

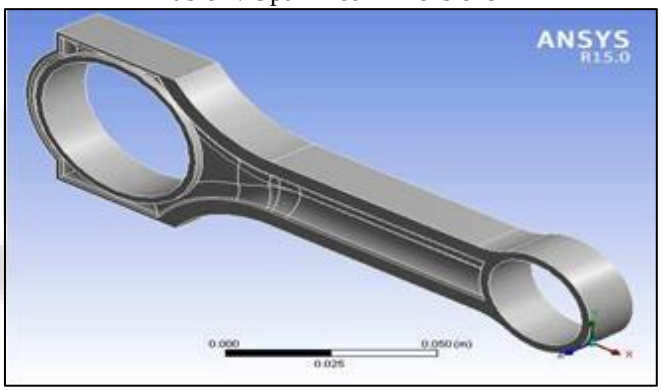

Fig. 8: CAD Model of Connecting Rod total width 26mm with middle thickness 5.5mm & side width 6.0

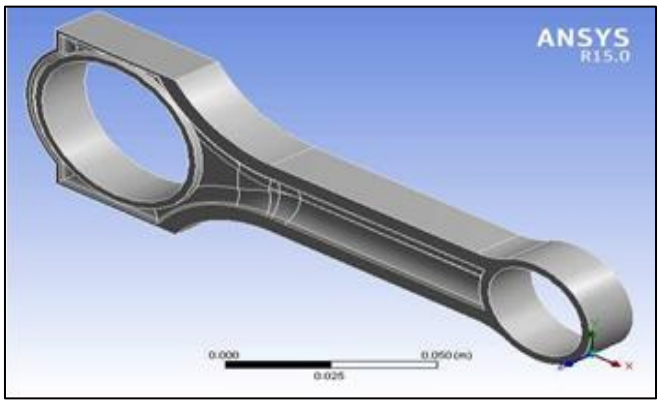

Fig. 9: CAD Model of Connecting Rod total width 25mm with middle thickness 5.4mm & side width 6.1

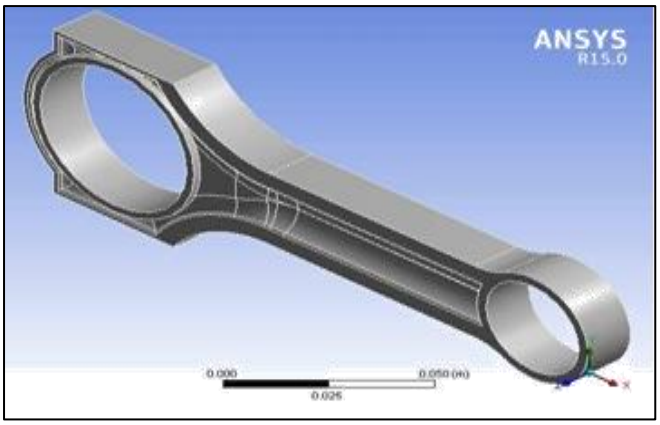

Fig. 10: CAD Model of Connecting Rod total width 24mm with middle thickness 5.3mm & side width 6.2

1) Material Property of C70S6

Young's modulus	210000Mpa
Poission's ratio	0.3
Density	7850 kg/m3
Compressive yield strength	920Mpa
Compressive ultimate strength	600Mpa

Table 3:

VI. RESULT ANALYSIS AND DISCUSSION

A. Validation of the Experimental Result

The validation of the Experimental result is done by carrying out the simulation work on the Ansys Static Structural and Linear Buckling (Coupled) 15.0 Work bench.

B. Experimental and Simulation Result

Critical buckling stress prediction: Classical buckling analysis

1) Euler's formula

$$\sigma_{cr}^{e} = (\pi\text{^}2\ E)/\ ((K_y\ L)/r_y)^2 \ldots (1)$$

Where E is the elastic modulus, Ky is 0.5 for a fixed–fixed joint effective length L, radius of gyration r this formula is used to analyze classical buckling for symmetrical column

2) Rankine formula

$$\sigma_{cr} = \left(\frac{1}{\sigma_{cr}^{e}} + \frac{1}{\sigma_{cr}^{p}}\right)^{-1} \ldots\ldots\ldots (2)$$

Where is Euler formula, yield strength this formula is used to analyze classical Buckling for unsymmetrical column

3) Buckling Prediction Via Finite Element Analysis

$$\sigma_{fem} = \frac{\text{Load Multiplier} \times \text{Applied Static Load}}{\text{Area}} \ldots\ldots (3)$$

C. Stress Prediction Via Finite Element Analysis

Critical buckling is analyzed by Euler's formula but connecting rod is unsymmetric section a rankine formula is used to predict buckling stresses to validate the value of load multiplier is evaluated by finite element method from ansys workbench and critical buckling stresses are calculated by equation no. (3)

D. Factor of Safety of Connecting Rod of Different Middle Thickness &Side Width of Shank Cross Section Area

$$\text{Factor of Safety} = \frac{\text{Ultimate Stress}}{\text{Allowable Stress}}$$

A static structural and linear buckling analysis (coupled) was carried out on C70S6 material connecting rod with different middle thickness &side width shank cross sectional area to determine the factor of safety and distribution of stresses along the effective length of the connecting rod. buckling stress distribution contours in case optimized connecting rod section area 26mm, 25mm, 24mm, 23mm, 22mm with different middle thickness & side width in each sectional area of connecting rod shank for the five different profiles are shown in Figures, and the effect of different shank area profiles on the buckling stress distribution for various shank cross sectional area are represented in the Figures.

It is evident that there is a decrement in the slenderness ratio and gradually increase in radius of gyration due to optimizing the connecting rod section by providing a variable middle thickness & side width of connecting rod shank sectional area in a different profile of connecting rod a width of cross sectional area of shank is reduced by 1mm and cross section is optimized by optimizing the parameters of cross section web ,on decreasing middle thickness and increasing side width of cross section radius of gyration increases due to this strength and durability increases but slenderness ratio decreases due to optimized side width of connecting rod cross sectional area of shank reduces stress concentration factor and increases factor of safety due to particle concentration in optimized-section is more than I-section ,Hence strength ,durability of connecting rod increases.

1) Vonmises Stress Distribution at various location of connecting rod of Different shank cross section area

A static structural and linear (coupled) analysis was carried out on C70S6 material connecting rod to determine the vonmises stress distribution at different locations.

2) Vonmises Stress distributions on side rear face of connecting rod of reduced shank sectional area:

Vonmises stress distribution contours in case of cross sectional area reduction for different profiles are shown in Figures 5.1-5.6. The effect of different profiles on the vonmises stress distribution various location are shown. From the Figures 14-16, it can be seen that the nature of the vonmises stress is compressive. A stresses developed at different locations of connecting rod of reduced cross sectional area It is also observed that the magnitude of the stress is maximum in the optimized-section of a connecting rod compared to I-section it could be analyzed that optimized-section is more durable than I-section

E. Observation Figure (Validation)

1) Buckling stresses

Thickness	Experimental Results	Simulation Results	Percentage Error
26	568	614	6%
25	564	608	6%
24	561	604	5%
23	554	596	5%
22	552	590	4%

Table 4: Experimental and Simulation Result for the Reduced cross section of Connecting rod.

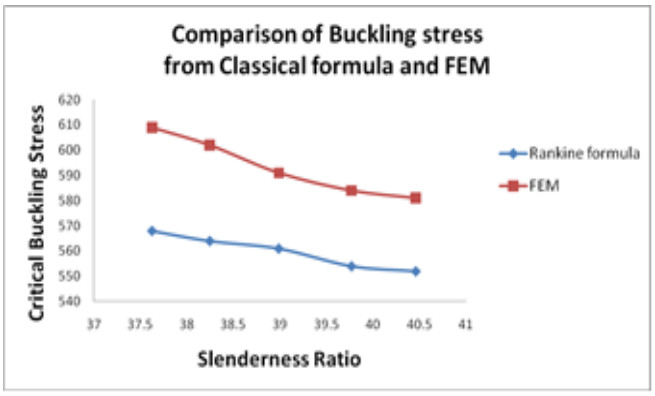

Fig. 11: Experimental and Simulation Result the Reduced cross section of Connecting rod

Figure shows Validation of experimental result between slenderness ratio and critical buckling stress of connecting rod by using rankine formula and FEM method.

Thickness	Optimized-cross section	I-Cross section
26	614	609
25	608	602
24	604	591
23	596	584
22	590	581

Fig. 5: Optimized cross section and I-Cross Section Result of the Connecting rod.

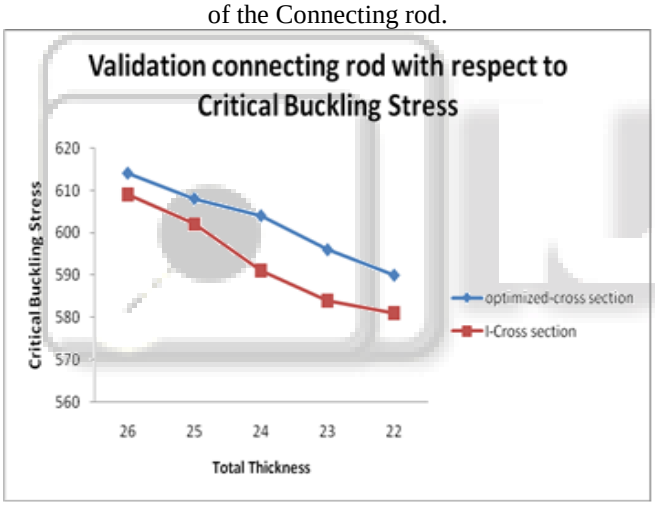

Fig. 12: Validation of Optimized cross section and I-Cross Section Result of the Connecting rod.

Allowable Stress I -Section					
Thickness	Critical Buckling Stress	Allowable Stress			
		Location-1	Location-2	Location-3	Location-4
22	609	196.89	238.33	235.48	271.66
23	602	198.2	244.86	238.49	273.48
24	591	202.68	247.39	241.46	276.66
25	584	207.36	251.66	244.68	279.43
26	581	210.58	253.43	248.88	281.98

Table 6: Simulation Result Allowable stress for the Connecting rod of I-section

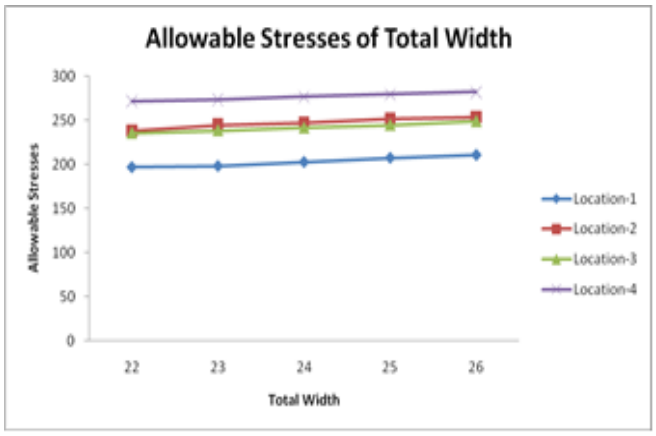

Fig. 13: Validation of Allowable Stress of I-Cross Section of the Connecting rod

Factor of Safety (Validation)			
Location-1	Location-2	Location-3	Location-4
3.09	2.55	2.58	2.24
3.03	2.45	2.52	2.2
2.91	2.38	2.44	2.13
2.81	2.32	2.38	2.08
2.75	2.29	2.33	2.06

Table 7: Validation of experimental result of allowable result of different location of connecting rod

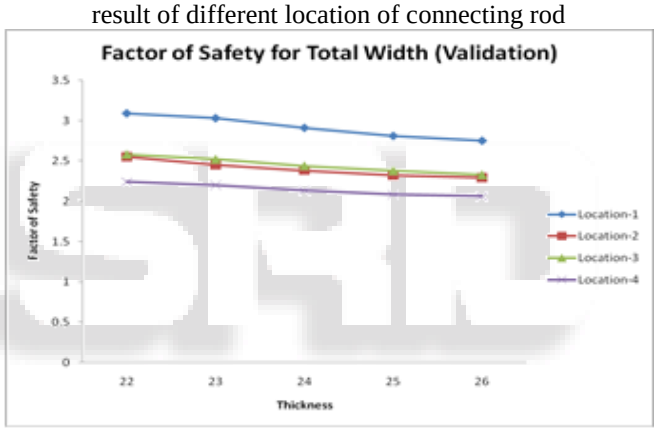

Fig. 14: Validation result of factor of safety of I-Cross Section of the Connecting rod

Above Figure and graph shows a validation of experimental result of connecting rod of allowable stresses and factor of safety results and also shows a comparison of rankine formula, slenderness ratio with finite element analysis to validate a present model for further optimization and analysis of factor of safety for safe design. It was also predicted that on above validation critical buckling stress of optimized section of connecting rod is more so that it has tendency to bear high amount of load.

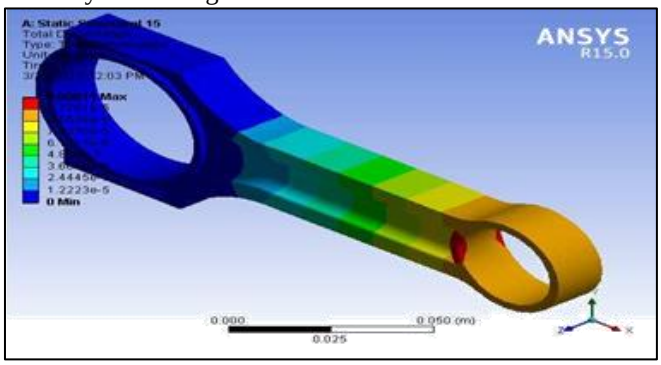

Fig. 15: Total Deformation of I-section Connecting rod width 26mm

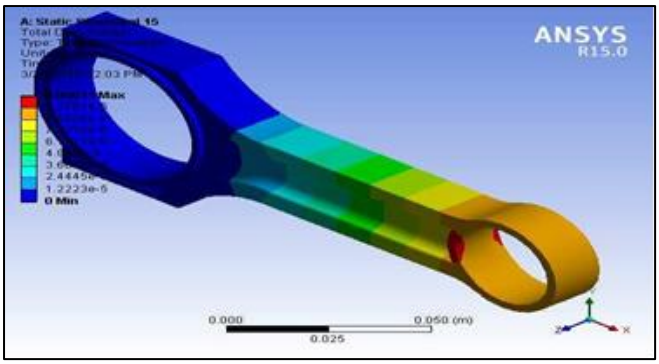

Fig. 16: Total Deformation of I-section Connecting rod width 25mm

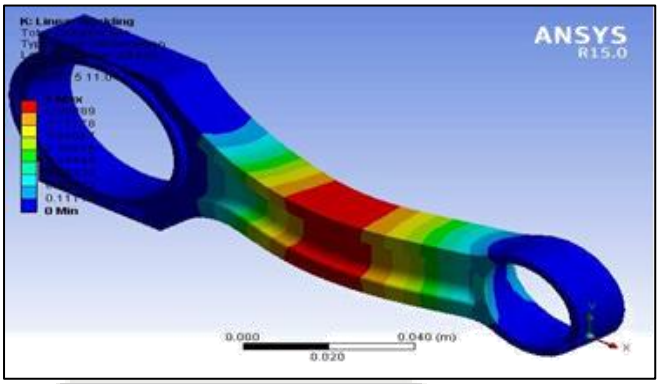

Fig. 17: Critical Buckling of I-section Connecting rod width 23mm

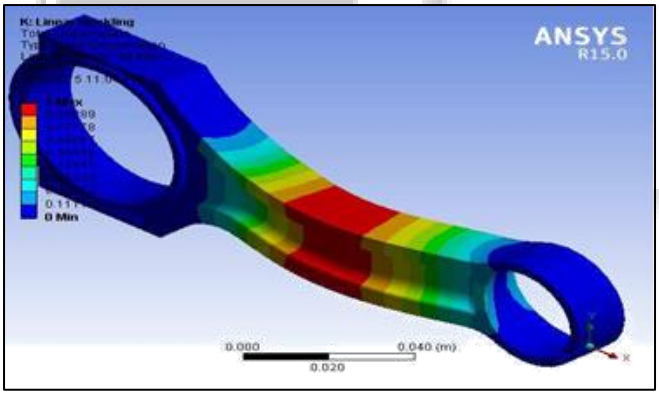

Fig. 18: Critical Buckling of I-section Connecting rod width 23mm

2) Optimization Results

Optimized Dimensions		Optimized I -Section					
				Allowable Stress			
Middle Thickness	Side Thickness	Thickness	Critical Buckling Stress	Location-1	Location-2	Location-3	Location-4
5.5	6	26	614	199.46	241.66	237.84	274.79
5.4	6.1	25	608	202.44	247.8	240.94	276.84
5.3	6.2	24	604	205.49	250.68	243.64	279.7
5.2	6.3	23	596	208.44	254.36	246.86	283.34
5.1	6.4	22	590	214.98	256.79	253.89	286.89

Table 8: Simulation Result Allowable stress for the Connecting rod of optimized-section

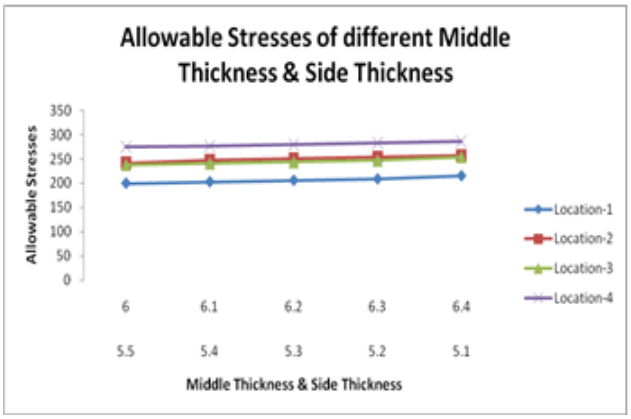

Fig. 19: Optimization result of Allowable stress of optimized-Cross Section of the Connecting rod of Middle Thickness & Side Thickness.

Factor of Safety (Optimization)			
Location-1	Location-2	Location-3	Location-4
3.07	2.54	2.58	2.23
3	2.45	2.52	2.19
2.93	2.4	2.47	2.15
2.85	2.34	2.41	2.1
2.74	2.29	2.32	2.05

Fig. 9: Simulation Result Allowable stress for the Connecting rod of Middle Thickness & Side Thickness

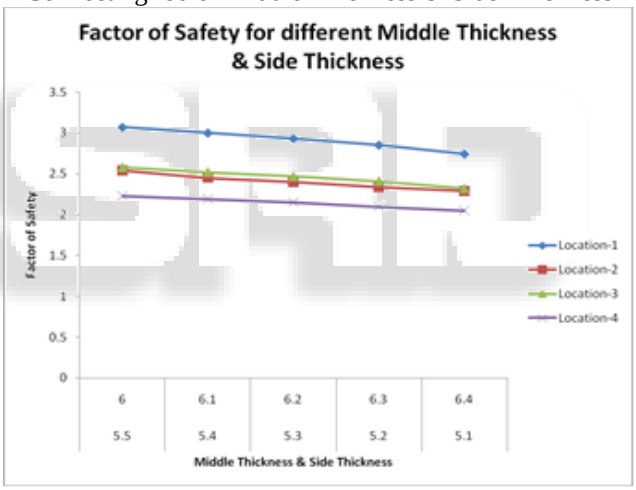

Fig. 20: Optimization result of Allowable stress of optimized-Cross Section of the Connecting rod of Middle Thickness & Side Thickness

Thickness	Rankine formula	Optimized-cross section	Percentage error
26	568	614	-0.074918567
25	564	608	-0.072368421
24	561	604	-0.071192053
23	554	596	-0.070469799
22	552	590	-0.06440678

Fig. 10: Simulation Result for the reduced cross section of Connecting rod of I-section and optimized-section

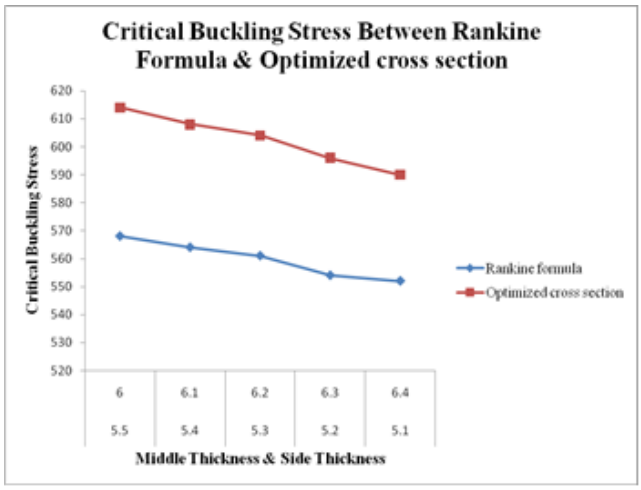

Fig. 21: Rankine formula and Simulation Result of the optimized cross section of Connecting rod.

Above Figures and graphs shows an optimization of experimental result of connecting rod of allowable stresses and factor of safety results as well as comparison of critical buckling stress with rankine formula.

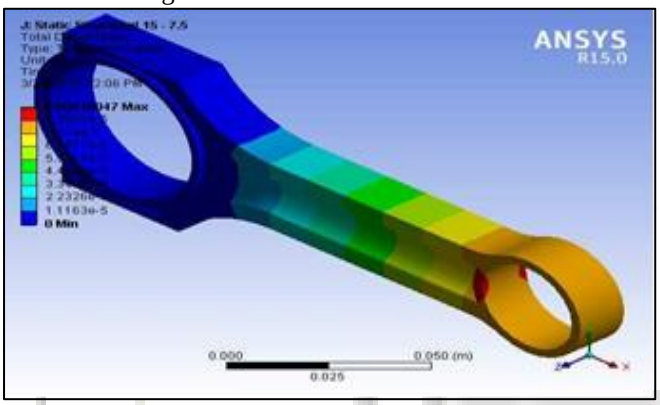

Fig. 22: Total Deformation of Optimized I- Section Connecting rod width 26mm and different middle thickness & side width

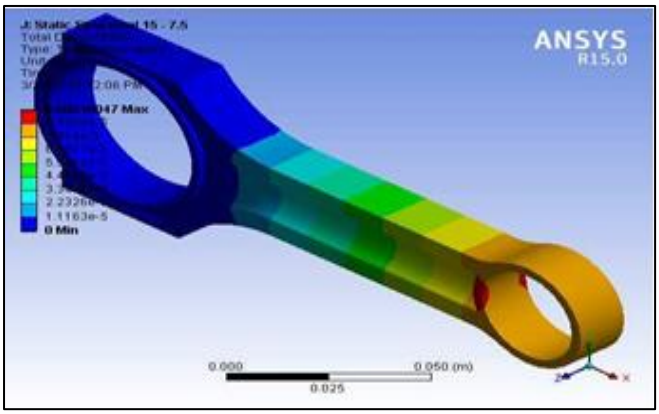

Fig. 23: Total Deformation of Optimized I- Section Connecting rod width 25mm and different middle thickness & side width

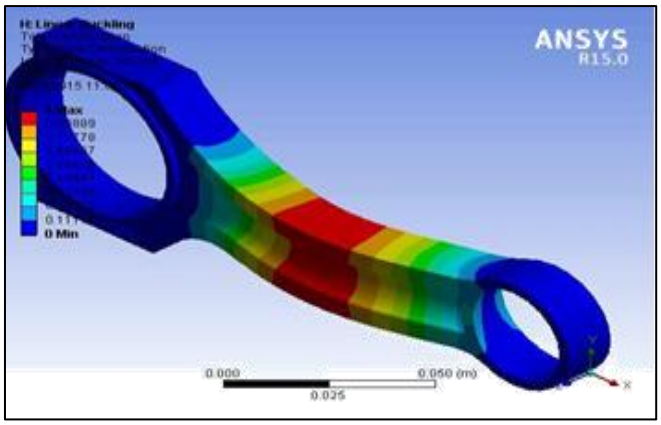

Fig. 24: Critical Buckling of Optimized I- Section Connecting rod width 25mm and different middle thickness & side width

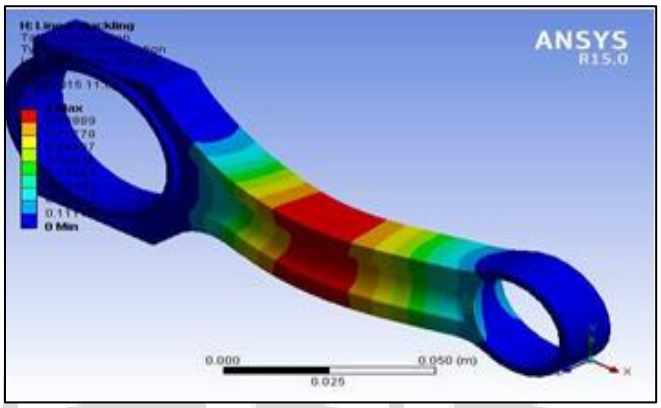

Fig. 25: Critical Buckling of Optimized I- Section Connecting rod width 24mm and different middle thickness & side width

VII. CONCLUSION

The current analysis has presented a study of factor of study characteristics of a connecting rod of different profiles. Coupled-field analysis was carried out on C70S6 system. The effect of different middle thickness & side width of the connecting rod with middle thickness (5.5,5.4,5.3,5.2,5.1) & side width (6.0,6.1,6.2,6.3,6.4) on the factor of safety, critical buckling stress and allowable stress at different location of C70S6 material effects variations along the connecting rod was studied. From the analysis of the results, following conclusions could be drawn.

A. Influence of Different Middle Thickness & Side Width

- The factor of safety along the connecting rod profile is found to be maximum of the location-1 profile near small end with middle thickness & side width and increases along the side width up to the connecting rod for all the five profiles. The critical buckling stress distribution along the length and middle portion of a connecting rod and mid shank of a connecting rod is maximum.
- The magnitude of the critical buckling stress is minimum in the case of middle thickness (5.1) & side width (6.4) C70S6 material profile with connecting rod of middle thickness (5.5,5.4,5.3,5.2,5.1) & side width (6.0,6.1,6.2,6.3,6.4). The nature of the critical buckling stress is maximum at middle thickness (5.5) & side width (6.0).

- The nature of the allowable stress is maximum near location - 4 of connecting rod and changes with respect to connecting rod profile towards the small end of the connecting rod for all the profiles of connecting rod.
- In a comparison with the middle thickness & side width connecting rod with respect to present model resulted in higher factor of safety, critical buckling stress characteristics close to the small end of the connecting rod for a different profile. The allowable stresses are greater on present model in comparison with optimized model of connecting rod.
- The comparative results for selected parameters showed that the factor of safety characteristics of the connecting rod of C70S6 is best for a different angle profile with middle thickness (5.5,5.4,5.3,5.2,5.1) & side width (6.0,6.1,6.2,6.3,6.4) the operating parameter. Connecting rod with middle thickness (5.4mm) & side width (6.1mm). Angle profile is nearly as economic as the profile of minimum material requirement and the construction cost is also less compared with other connecting rod. Hence middle thickness (5.4mm) & side width (6.1mm) profile is attractive because for higher Factor of safety at each location it requires much less volume than other profile.

VIII. FUTURE SCOPE

1) Further analysis could be done for variable materials and connecting rod profiles.
2) Analysis could be done to predict frequency of connecting rods of different profiles.
3) CFD simulation could be done for present analysis to predict wall fluxes due to lubrication on connecting rod.
4) Vibration analysis can also be done with considering rotation speed and fluid pressure on assembled connecting rod.
5) Forced vibration analysis is also possible for present connecting rod profile.
6) Crack propagation i.e. internal & external crack effect on connecting rod could be predicted for present model.

REFERENCES

[1] H. Grass, C. Krempaszky *, E. Werner "3-D FEM-simulation of hot forming processes for the production of a connecting rod" Computational Materials Science 36 (2006) 480–489.
[2] S. Griza *, F. Bertoni, G. Zanon, A. Reguly, T.R. Strohaecker "Fatigue in engine connecting rod bolt due to forming laps" Engineering Failure Analysis 16 (2009) 1542–1548.
[3] Moon Kyu Lee a, Hyungyil Lee a,*, Tae Soo Lee a, Hoon Jang b "Buckling sensitivity of a connecting rod to the shank sectional area reduction" Materials and Design 31 (2010) 2796–2803.
[4] Liming Zheng, ShuqingKou, Shenhua Yang, LiliLi, FeiLi "A study of process parameters during pulsed Nd:YAG laser notching of C70S6 fracture splitting connecting rods" Optics & Laser Technology 42 (2010) 985–993.
[5] Vanluu Dao, Shengdun Zhao n, Wenjie Lin, Chenyang Zhang "Effect of process parameters on microstructure and mechanical properties in AlSi9Mg connecting-rod fabricated by semi-solid squeeze casting" Materials Science & Engineering A 558 (2012) 95–102.
[6] Saharash Khare, O.P. Singh, K. Bapanna Dora, C. Sasun "Spalling investigation of connecting rod" Engineering Failure Analysis 19 (2012) 77–86.
[7] Xianghui Meng a,b,n, YoubaiXie a,b "A new numerical analysis for piston skirt–liner system lubrication considering the effects of connecting rod inertia" Tribology International 47 (2012) 235–243.
[8] S B Chikalthankar*, V M Nandedkar**, Surendra Prasad Baratam* "Fatigue Numerical Analysis for Connecting Rod" International Journal of Engineering Research and Applications (IJERA) ISSN: 2248-9622.
[9] Prof. N.P.Doshi, Prof .N.K.Ingole "Analysis of Connecting Rod Using Analytical and Finite Element Method" International Journal of Modern Engineering Research (IJMER) www.ijmer.com Vol.3, Issue.1, Jan-Feb. 2013 pp-65-68.
[10] Bai-yan He a,, Guang-da Shi a, Ji-bing Sun b, Si-zhuan Chen a, Rui Nie a "Crack analysis on the toothed mating surfaces of a diesel engine connecting rod" Engineering Failure Analysis 34 (2013) 443–450.
[11] G. Naga Malleshwara Rao "Design Optimization and Analysis of a Connecting Rod using ANSYS" International Journal of Science and Research (IJSR), India Online ISSN: 2319-7064.
[12] Leela Krishna Vegi, Venu Gopal Vegi " Design And Analysis of Connecting Rod Using Forged steel" International Journal of Scientific & Engineering Research, Volume 4, Issue 6, June-2013 ISSN 2229-5518.
[13] Y.J. Zhang*, H.P. Luo, G.X. Liu, Z.N. Guo, Y.J. Tang "Research on power supply and control system of WEDM cutting of stress-notches in fracture splitting processing of connecting rod" Procedia CIRP 6 (2013) 250 – 254.
[14] Kuldeep B1, Arun L.R2, Mohammed Faheem3 "Analysis And Optimization Of Connecting Rod Using Alfasic Composites" International Journal of Innovative Research in Science, Engineering and Technology Vol. 2, Issue 6, June 2013.
[15] Ling Li ⇑, Rong Wang "Failure analysis on fracture of worm gear connecting bolts" Engineering Failure Analysis 36 (2014) 439–446.
[16] WeijunHUI１, SilianCHEN２, ChengweiSHAO１, YongjianZHANG１, HanDONG２ "Hot Deformation Behavior of Vanadium micro alloyed Medium carbon Steel for Fracture Splitting Connecting Rod" JOURNAL OF IRON AND STEEL RESEARCH,INTERNATIONAL□２０１５,２２(７): ６１５G６２１.
[17] Mr. J.D.Ramani*, Prof. Sunil Shukla**, Dr. Pushpendra Kumar Sharma "FE-Analysis of Connecting Rod of I.C.Engine by Using Ansys for Material Optimization" Mr. J.D.Ramani et al Int. Journal of Engineering Research and Applications www.ijera.com ISSN : 2248-9622, Vol. 4, Issue 3(Version 1), March 2014, pp.216-220.
[18] Mohammed Mohsin Ali Ha, Mohamed Haneef b* "Analysis of Fatigue Stresses on Connecting Rod Subjected to Concentrated Loads At The Big End" Materials Today: Proceedings 2 (2015) 2094 – 2103.

[19] J.P. Fuertesa, O. Murilloa, J. Leóna,*, C. Luisa, D. Salcedoa, I. Puertasa, R. Luria "Mechanical properties analysis of an Al-Mg alloy connecting rod with submicrometric structure" Procedia Engineering 132 (2015) 313 – 318.
[20] D.Gopinatha,Ch.V.Sushmab* "Design and Optimization of Four Wheeler Connecting Rod Using Finite Element Analysis" Materials Today: Proceedings 2 (2015) 2291 – 2299.
[21] He Zhenpeng et.al. "Tribilogical performances of connecting rod and by using orthogonal experiment, regression method and response surface methodology" http://dx.doi.org/10.1016/j.asoc.2015.01.009.
[22] Yu Wang a, Feng-Ming Li a "Nonlinear dynamics modeling and analysis of two rods connected by a joint with clearance" http://dx.doi.org/10.1016/j.apm.2014.10.056.
[23] Puran Singh1, Debashis Pramanik2, Ran Vijay Singh3 "Fatigue and Structural Analysis of Connecting Rod's Material Due to (C.I) Using FEA" International Journal of Automotive Engineering and Technologies Vol. 4, Issue 4, pp. 245– 253,2015.
[24] J.P. Fuertes1, C.J. Luis2, R. Luri3, D. Salcedo4, J. León5, I. Puertas∗,6 "Design, simulation and manufacturing of a connecting rod from ultra-fine grained material and isothermal forging" Journal of Manufacturing Processes 21 (2016) 56–68.
[25] C. Juarez a, F.Rumiche a,*, A.Rozas a, J.Cuisano b, P.Lean b "Failure analysis of a diesel generator connecting rod" Case Studies in Engineering Failure Analysis 7 (2016) 24–31.

